Molecular beam epitaxy regrowth and device performance of GaAs-based pseudomorphic high electron mobility transistors using a thin indium passivation layer

SHEU-SHUNG CHEN, CHIEN-CHENG LIN
Department of Materials Science and Engineering, National Chiao Tung University, Hsinchu 300, Taiwan
E-mail: chienlin@cc.nctu.edu.tw

CHIN-KUN PENG
Procomp Informatics Ltd., Hsinchu 300, Taiwan

YI-JEN CHAN
Department of Electrical Engineering, National Central University, Chungli 32054, Taiwan

Using the technique of molecular beam epitaxy, an indium passivation layer as thin as several tens of Å was implemented to protect underlying III-V epilayers from carbon and oxygen contamination. After the subsequent desorption of the passivation layer, GaAs-based pseudomorphic high electron mobility transistors (PHEMTs) were regrown. Negligible residual carriers were detected at the interface between the regrown PHEMTs and the underlying layer, resulting in a superior performance. The regrown PHEMTs with a $1 \times 100\,\mu m^2$ gate demonstrated an extrinsic transconductance g_{me} as high as $330\,mS\,mm^{-1}$. Microwave measurements showed that the current gain cut-off frequency f_t was 26.5 GHz and the maximum oscillation frequency f_{max} was up to 48 GHz. A small-signal equivalent circuit model of the regrown PHEMTs was also evaluated.

1. Introduction

Molecular beam epitaxy (MBE) is a powerful technique in the development of III-V compound semiconductor devices. Among these devices, optoelectronics have attracted a great deal of attention due to their extensive commercial applications. As progress continues, the increasing demands for more multi-functional circuits create an overload in device fabrication. While direct epitaxial growth cannot meet these demands, the regrowth technique becomes an alternative to facilitate the device process and make possible a further improvement in performance. There are several methods for the regrowth of III-V epilayers, including arsenic passivation at low substrate temperatures [1–3], sulfur-based chemical treatments [4–6], and patterned regrowth [7, 8], etc. Each meets certain levels of success and deficiency. All these studies focused on retaining an interface of high-quality between the originally grown and regrown layers. The high purity at the interface is beneficial to the regrowth technique. A clean defect-free interface is ideal for the reliability of the regrown devices. Such a regrowth technique can relieve the growth burdens of complex multifunctional opto-electronic devices on the same wafer and improve the flexibility in device fabrication.

To develop a simple regrowth technique without any modification of the commercial MBE system is of great interest. Although previous studies indicated that the thin arsenic layers, condensed *in situ* below room temperature, could lead to good cleanliness at the interface, there were still some limitations to the rapid cooling of the substrate in a modern MBE system design. To obtain a good regrown sample, the passivation layer is crucial in two respects. First, it must be thick enough to prevent the residual carbon and oxygen species from contaminating the underlying epilayers after exposure to the atmosphere for further processing. Secondly, it should be thin enough to be easily removed. Based on these criteria, indium was considered a suitable passivation source, which could be condensed above room temperature.

In the present study, pseudomorphic high electron mobility transistors (PHEMTs) were regrown *in situ* in the MBE chamber after thermally desorbing the indium passivation layer, which was previously deposited on the buffer layer of the GaAs substrate. The potential contamination of carbon and oxygen from air at the interface was examined using X-ray photoemission spectroscopy (XPS). The *C–V* depth profiler was used to determine the carrier concentration at the interface between the regrown PHEMTs and the underlying layer.

The d.c. and microwave characteristics were examined to evaluate the performance of the regrown PHEMTs. Finally, a small-signal equivalent circuit model of the regrown PHEMTs was simulated.

2. Experimental

Fig. 1 illustrates the regrowth sequences for the PHEMT device using a MBE system (Model 32P, Riber). The epi-ready semi-insulating (100) GaAs substrate was loaded into the MBE system. The water vapor was desorbed at 350 °C in the transfer chamber, followed by a normal degassing in the growth chamber from a preset temperature (300 °C) to 630 °C with a slow heating rate. After growing a 0.5 μm-thick GaAs buffer layer at 580 °C under an As-stabilized condition, gallium and arsenic sources were abruptly shuttered to terminate the growth and the substrate temperature was lowered to 50 °C for the further deposition of a thin indium layer, as shown in Fig. 1a. The In-passivated sample was then removed from the MBE system and preserved in air for weeks before being reloaded for regrowth. Fig. 1b represents the thermal desorption of the indium passivation layer at 630 °C for 30 min. During the thermal desorption process, indium, carbon and oxygen were monitored using a residual gas analyzer (RGA). When none of these species were able to be detected the clear GaAs(100) $-$ (2 $\times$ 4) surface reconstruction was obtained under an As-stabilized condition monitored by reflection high energy electron diffraction (RHEED), indicating that the indium layer was completely removed with no contamination of carbon and oxygen in the underlying layers. Fig. 1c reveals that the regrown PHEMTs consist of a 0.5 μm undoped GaAs buffer layer, a 15 nm undoped $In_{0.15}Ga_{0.85}$ As pseudomorphic channel layer, a 3 nm undoped $Al_{0.25}Ga_{0.75}As$ spacer layer, a 50 nm Si-doped $Al_{0.25}Ga_{0.75}As$ gate layer with 2×10^{18} cm^{-3} doping concentration, and a 20 nm Si-doped GaAs cap layer with 3×10^{18} cm^{-3} doping concentration. The PHEMTs were regrown at 580 °C, except that the $In_{0.15}Ga_{0.85}As$ channel layer was processed at 540 °C. The regrown PHEMTs had a typical oval-defect density ranging from 10^2 to 10^5 cm^{-2} and the featureless specular surface was similar to that of the traditional process with no passivation layer. Mesa etching was then performed using a phosphoric-based etchant, and the source and drain ohmic metal patterns were defined photo-lithographically, followed by the evaporation and lift-off of AuGe/Ni/Au metals. The Al gate was formed after the gate recess process.

The surface compositional profiles of the In-passivated sample were measured using electron spectroscopy for chemical analysis (ESCA: model PHI-5400, Perkin-Elmer). The MgK_α X-ray source was operated at 300 W and 15 keV, while the specimen was sputtered by argon ions. The *C–V* profiles were plotted using an electro-chemical system (Model PN-4300, Bio-Rad) to determine the carrier concentration at the interface between the original buffer layer and the regrown PHEMTs.

Based on the Hall effect, with a van der Pauw configuration, the carrier concentration and the electron mobility in the regrown PHEMTs with 4×5 mm^2 dimensions were measured at a magnetic field of 0.5 T and an electric current of 100 μA. The device d.c. characteristics with a 1×50 μm^2 gate and a source–drain spacing of 3 μm were explored using a semiconductor parameter analyzer (Model 4145B, Hewlett Packard). The microwave scattering parameters (*S*-parameter) were measured in the range of 0.45 to 26.5 GHz with a microwave probe station (CASCADE) and an automatic network analyzer (Model 8510C, Hewlett Packard). A small-signal equivalent circuit was also simulated based on the measured *S*-parameters with a microwave design system (MDS: Hewlett Packard).

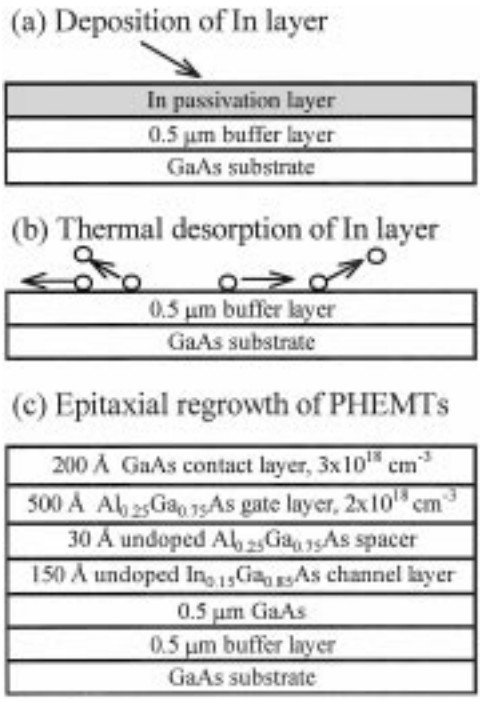

Figure 1 Regrowth sequences of PHEMTs. Both the In deposition and desorption were completed in the MBE growth chamber.

3. Results and discussion

The electron energies of As_{3d}, Ga_{2p}, In_{3d}, O_{1s}, and C_{1s} core levels were monitored by XPS analyzes. Fig. 2

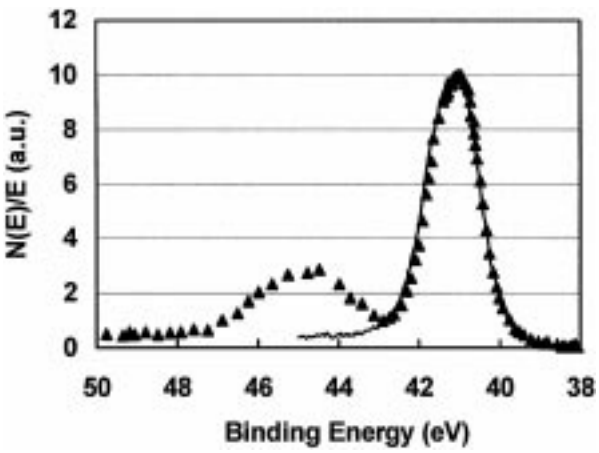

Figure 2 XPS spectra near the As_{3d} core energy for the surfaces of the as-grown In-passivated sample (▲) and that after being sputtered for 3 min (solid line).

TABLE I XPS depth profiles of the In-passivated samples with a 0.5 μm-thick GaAs buffer layer.

Sputter time (min)	C_{1s}	O_{1s}	Ga_{2p3}	As_{3d}	In_{3d5}
0	21.3	30.5	—	14.5	33.6
1	—	9.5	28.7	26.2	35.5
3	—	—	62.3	31	6.6
8	—	—	66.7	31.3	1.8
10	—	—	67.9	31.5	0.5
15	—	—	69.3	30.6	—
25	—	—	69.3	30.6	—

shows the XPS spectra near the As_{3d} core energy for the surfaces of the as-grown In-passivated sample and the one after being sputtered for 3 min, respectively. The oxide peak almost completely disappeared after being sputtered for 3 min. Details of the resultant depth profiles are listed in Table I. It is shown that carbon and oxygen existed only near the outermost surface. Both elements were effectively prevented from contaminating the underlying epilayers due to the indium layer. The simultaneous appearance of In_{3d} and Ga_{2p} signals indicates that the indium layer was not as smooth as expected. The early appearance of the As_{3d} signal was probably caused by a high arsenic background during the MBE growth of the indium layer.

Fig. 3 shows the *C–V* depth profile of the regrown PHEMTs with a total thickness of 0.6 μm, which covered the regrowth layers. Near the outermost surface layer, the n-type carrier concentration was $3 \times 10^{18}\,cm^{-3}$, which was very close to the expected value. The concentration then rapidly decreased to as low as $2 \times 10^{14}\,cm^{-3}$ at the interface between the original buffer layer and the regrown PHEMTs, similar to the concentration in the semi-insulating substrate, indicating that no residual carriers existed at the interface. This *C–V* depth profile shows no perceivable difference from that of conventional PHEMTs. Both XPS and *C–V* results reveal that a high-quality interface was preserved by the indium passivation layer.

Van der Pauw Hall measurements on the regrown samples showed two-dimensional electron concentrations of 4.4×10^{12} and $4.0 \times 10^{12}\,cm^{-2}$, and electron mobilities of 4300 and $15\,400\,cm^2\,V^{-1}\,s^{-1}$ at room temperature and 77 K, respectively. These values are consistent with those of the traditionally grown PHEMTs. The high carrier concentration and good electron mobility ensure the superior performance of PHEMTs as described later.

Fig. 4a shows the d.c. characteristics for regrown PHEMTs with a $1.0 \times 50\,\mu m^2$ gate at 300 K, indicating a good pinch-off at a gate bias of -1.0 V. The extrinsic transconductance g_{me} of $330\,mS\,mm^{-1}$ was obtained at $V_{ds} = 1.75$ V and $I_{ds} = 136\,mA\,mm^{-1}$, as shown in Fig. 4b. With a measured source resistance R_s of $0.2\,\Omega\,mm$, the estimated intrinsic transconductance g_{mi} was $353\,mS\,mm^{-1}$. These results were better than those of the conventional PHEMTs mentioned in a previous study [9].

Microwave *S*-parameters for the devices with a $1 \times 100\,\mu m^2$ gate were measured at frequencies ranging from 0.45 to 26.5 GHz biased at $V_{ds} = 2.0$ V and $V_{gs} = -0.25$ V. Fig. 5 displays the maximum available gain (MAG), maximum stable gain (MSG), and current gain $|h_{21}|^2$, calculated from the measured *S*-parameters. The current gain cut-off frequency f_t was estimated at

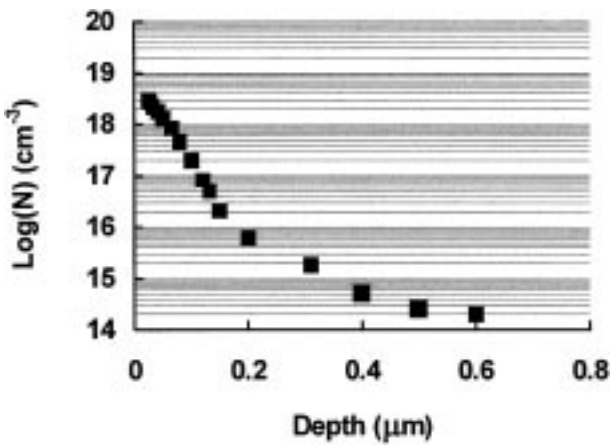

Figure 3 *C–V* depth profiles of the regrown PHEMTs.

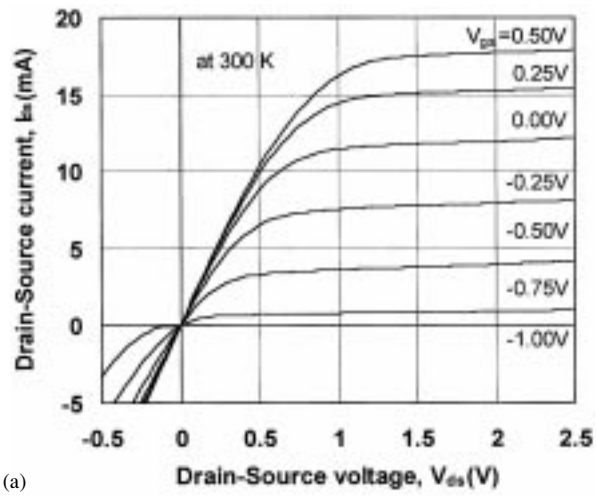

(a)

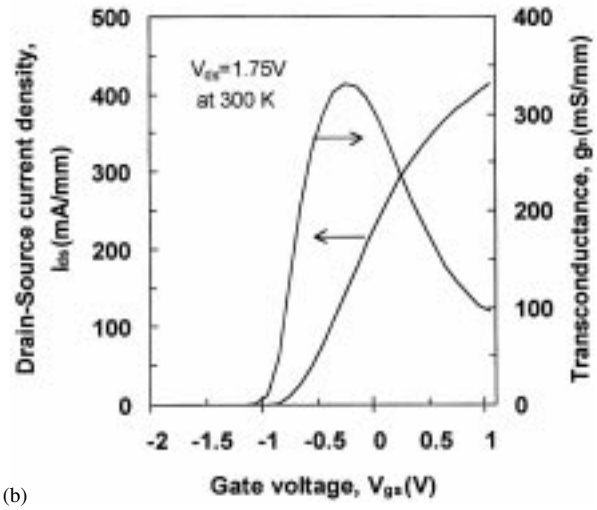

(b)

Figure 4 D.c. *I–V* characteristics of the regrown PHEMT device with a 1.0 μm gate length at 300 K. (a) $I_{ds} - V_{ds}$; (b) $I_{ds} - g_{me} - V_{gs}$.

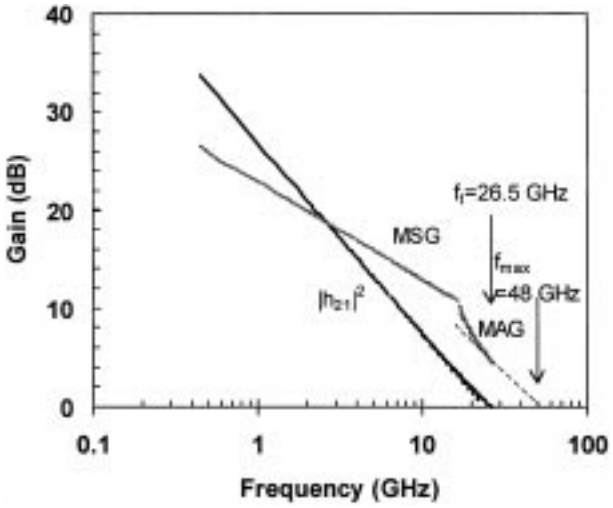

Figure 5 Microwave characteristics of the regrown PHEMT device with a 1.0 μm-long gate at the frequencies ranging from 0.45 to 26.5 GHz at 300 K.

26.5 GHz by the unity gain intercept of the $|h_{21}|^2$ values. The maximum oscillation frequency $f_{\max}$ was about 48 GHz from the unity gain intercept of the MSG/MAG curves using a rate of 6 dB per octave roll-off.

Fig. 6 shows the small-signal equivalent circuit model of the regrown PHEMTs using the MDS to fit the measured *S*-parameters. Fig. 7 indicates an excellent agreement between the simulated and measured *S*-parameters ranging from 0.45 to 26.5 GHz. Table II lists the final element values for the equivalent circuit in Fig. 6. The simulated g_{mi} $(334\,\mathrm{mS\,mm^{-1}})$ and R_s $(0.1996\,\Omega\,\mathrm{mm})$ were consistent with the results obtained from the d.c. measurements (Fig. 4). The input capacitance C_{gss} $(1.97\,\mathrm{pF\,mm^{-1}})$ was small enough to ensure a better intrinsic transconductance g_{mi} and consequently improved the current gain cut-off frequency f_t. Moreover, the feedback capacitance C_{gd} $(0.25\,\mathrm{pF\,mm^{-1}})$ was so small that this device should be able to operate more stably. Meanwhile, the output conductance $g_o(=1/R_{ds})$ was $14.02\,\mathrm{mS\,mm^{-1}}$, resulting in a gain ratio g_{mi}/g_o of 23.8. Based on this small-signal equivalent circuit model, the microwave devices and other related sub-systems, including the matching network of this regrown PHEMT, could be better designed and correctly applied.

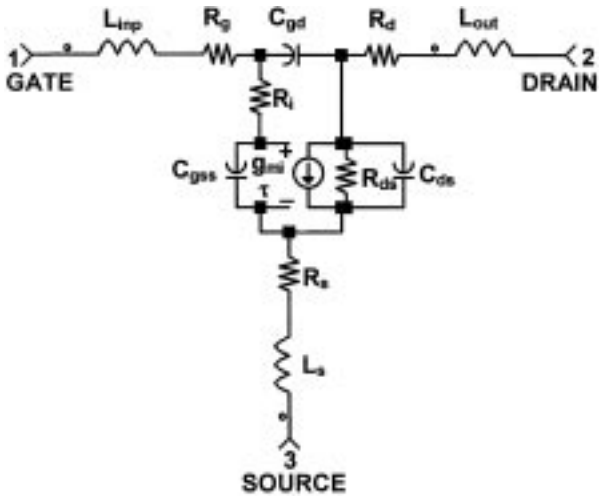

Figure 6 A typical small-signal equivalent circuit model of the regrown PHEMT device simulated by the HP MDS.

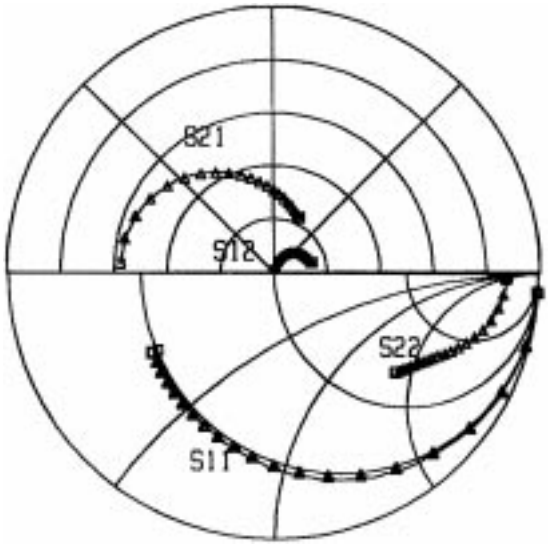

Figure 7 The measured *S*-parameters (solid line) and simulated data (△) from the small-signal equivalent circuit of the regrown PHEMT device ranging from 0.45 to 26.5 GHz. In the upper polar chart, the full scales of coordinate for S12 and S21 are one and five (arbitrary units), respectively. In the lower Smith chart, both S11 and S22 have the same co-ordinate scale equal to one (arbitrary unit).

TABLE II The final values of small-signal equivalent circuit elements for the regrown PHEMTs with a $1 \times 100\,\mu\mathrm{m}^2$ gate

Equivalent circuit element	Final value
Gate resistance R_s (Ω)	6.747
Source resistance R_d (Ω)	1.996
Drain resistance R_d (Ω)	6.011
Output resistance R_{ds} (Ω)	713.1
Intrinsic input resistance R_d (Ω)	8.936
Input capacitance C_{gds} (pF)	0.197
Feedback capacitance C_{gd} (pF)	0.025
Output capacitance C_{ds} (pF)	0.014
Input inductance L_{inp} (nH)	0.058
Source inductance L_d (nH)	0.00357
Output inductance L_{out} (nH)	0.0808
τ (ps)	1.26
g_{me} (mS)	33.4

4. Conclusions

Using a thin indium layer for surface passivation, the regrowth of PHEMTs was carried out *in situ* without any modification of a commercial MBE system. XPS analyzes showed that this thin indium layer was thick enough to protect the underlying epilayers from carbon and oxygen contamination during exposure to the air. The C–V-depth profiles revealed that no residual carriers were distributed at the interface between the original buffer layers and the regrown PHEMTs, resulting in high performance of regrown PHEMTs.

The regrown devices exhibited an extrinsic transconductance g_{me} as high as 330 mS mm^{-1}. Microwave measurements showed that the current gain cut-off frequency f_t was 26.5 GHz and the maximum oscillation frequency f_{max} was up to 48 GHz. The *S*-parameters obtained from the simulation of a small-signal equivalent circuit model were consistent with the measured ones. This simulation is essential to the design of microwave devices of the regrown PHEMTs. Based on the excellent transport and device characteristics, the In-passivated technique could result in an ideal interface for the regrown PHEMTs, applicable to a variety of different device structures.

Acknowledgment

The authors thank the financial support by the National Science Council, Taiwan, under Grant No. NSC 87-2216-E009-014.

References

1. S. P. KOWALCZYK, D. L. MILLER, J. R. WALDROP, P. G. NEWMAN and R. W. GRANT, *J. Vac. Sci. Technol.* **19** (1981) 255.
2. D. L. MILLER, R. T. CHEN, K. ELLIOTT and S. P. KOWALCZYK, *J. Appl. Phys.* **57** (1985) 1922.
3. P. ETIENNE, P. ALNOT, J. F. ROCHETTE and J. MASSIES, *J. Vac. Sci. Technol. B* **4** (1986) 1301.
4. C. J. SANDROFF, R. N. NOTENBURG, J. C. BISCHOFF and R. BHAT, *Appl. Phys. Lett.* **51** (1987) 33.
5. Y. NANNICHI, J. FAN, H. OIGAWA and A. KOMA, *Jpn. J. Appl. Phys.* **27** (1988) 2367.
6. J. WANG, T. CHENG, P. H. BETON, J. J. HARRIS, E. BOWSER and C. T. FOXON, *Semicond. Sci. Technol.* **8** (1993) 2101
7. A. Y. CHO and W. C. BALLAMY, *J. Appl. Phys.* **46** (1975) 783.
8. Y. C. PAO, J. FRANKLIN and C. YUEN, *J. Cryst. Growth* **127** (1993) 892.
9. C. K. PENG, W. H. LAN, S. L. TU, S. J. YANG, S.S. CHEN and C. C. LIN, *Mater Chem. Phys.* **45** (1996) 92.

Received 7 January
and accepted 17 April 2000